The Role of Faceting in $\{10\bar{1}2\}$ Twin Nucleation

Christopher D. Barrett

Abstract

{1012} twinning is the most profuse twin mode in Mg and plays a major role in its plasticity and deformation. Identification of the mechanisms and locations of twinning nucleation is crucial to characterize the ensuing microstructural evolution and failure. Herein, we provide a new theory of hexagonal close-packed twin nucleation. In essence, the theory is that twins need a pre-existing interface upon which to grow. In the earliest stages of nucleation, this requirement implies that the twin must be able to facet onto the same plane as the local interface, whether it be a free surface, stacking fault, or grain boundary, and that the action of twinning must reduce the defect energy of the pre-existing structure in order to remain stable until it can grow large enough to emit disconnections. The theory is demonstrated on {1012} twin nucleation at grain boundaries and stacking faults in Mg via molecular dynamics.

Keywords

Twinning • Nucleation • Magnesium • Molecular dynamics

Introduction

$\{10\bar{1}2\}$ twinning is a dramatic plastic mechanism which is pervasive in hexagonal close-packed (hcp) materials. HCP materials play a critical role in many industries and hold potential for even greater market penetration if their properties can be further optimized. In particular, Ti and Mg alloys have better strength-to-weight ratios than Al or steel alloys, and thus are critical lightweight components. These materials often experience brittle failure due to twinning. This failure might be avoidable if the twinning process was fully understood. The twinning process induces a 90° rotation of the crystal lattice, dramatically altering the microstructure and critical resolved shear stresses (CRSSs) of other modes within the twinned region. In Mg, $\{10\bar{1}2\}$ twinning is so profuse that it often consumes the entire microstructure of heavily textured components. While the twinning process has been extensively studied over the last seventy years and many advances have been made, the nucleation process whereby these twins originate is still poorly understood.

Twin nucleation has been studied and discussed extensively since the 1950s. The simplest nucleation theory is that twins can spontaneously form in the crystal bulk by a uniform shape change in some region responding to applied load [1]. In contrast, others suggested that a pre-existing defect of some nature was necessary to catalyze the nucleation process [2, 3]. This was lent weight by observations of large scatter in the observed CRSSs for twinning and sensitivity to loading direction [3–6], indicating some non-Schmid behavior [7]. The theory of heterogenous twin nucleation was later extended into multiple forms involving prior slip or concomitant microslip [8–12], and dissociation of bulk dislocations into several twinning disconnections [13–21]. Recent advances have lent greater weight to these heterogenous theories than the homogenous nucleation idea [22–26], but the exact process is still not very well defined.

Wang has shown, [26–28], that $\{10\bar{1}2\}$ twins have a minimum stable size, based on density functional theory (DFT) and atomistic results. When a twin is generated from a zonal mechanism based on dissociation of a lattice dislocation, at least eight twinned layers are necessary to prevent the embryo from collapsing. Additional work based on electron back-scatter diffraction (EBSD) has shown that twins nucleate more frequently at low-angle grain boundaries than at high-angle grain boundaries indicating that something about the structure of low-angle grain boundaries encourages twin nucleation.

Finally, recent results using both molecular dynamics and transmission electron microscopy have shown that small

C. D. Barrett (✉)
Department of Mechanical Engineering, Mississippi State University, Starkville, MS 39762, USA
e-mail: barrett@me.msstate.edu

J. B. Jordon et al. (eds.), *Magnesium Technology 2020*, The Minerals, Metals & Materials Series, https://doi.org/10.1007/978-3-030-36647-6_21

twin embryos do not have the lenticular morphology most often seen at the EBSD scale, but instead are heavily faceted [29, 30]. These facets have been shown to significantly enhance the glissile nature of the twin by a complex interaction process between disclinations at facet junctions and twinning disconnections [31, 32]. Additional interactions have been observed with other defects such as basal dislocations which again enhance the twin mobility [33, 34]. From the shear plane view, four facets are visible for the $\{10\bar{1}2\}$ twin: the typical twin boundary $\{10\bar{1}2\}$, the conjugate twin boundary $\{10\bar{1}2\}$, the basal-prismatic boundary, and the prismatic-basal boundary. Additionally, several other facets are also active which are not visible from this projection [35].

This work uses molecular dynamics to spontaneously nucleate twins under stress in Mg. The nucleation process is carefully characterized to produce a new theory of twin nucleation which we expect to be applicable to all hcp materials. Both single crystal and bi-crystal simulations were used to identify common elements present in very different nucleation scenarios.

Methodology

A single crystal with dimensions of 156 nm by 61 nm by 9.7 nm was generated with free surfaces in all dimensions. The z-direction was the shear plane normal. A semi-spherical region of atoms was removed in the center of one of the narrow faces to concentrate the initial plasticity away from the box corners. Equilibration was performed for at least 10 ps at 50 K and terminated with a pressure below 100 MPa using LAMMPS [36]. A constant strain rate of $10^8 s^{-1}$ in uniaxial tension was applied in the $\langle 0001 \rangle$ direction to favor $\{10\bar{1}2\}$ twinning. An NVT ensemble was used with a EAM potential by [37].

The bi-crystal was generated with the $\{0\,0\,0\,1\}$ plane of the upper grain appended to the $\{10\bar{1}4\}$ plane of the lower grain, producing a misorientation of 25.1°. The $[1\bar{2}10]$ direction was the tilt axis and periodic conditions were applied in that direction with free surfaces in the other two directions. The dimensions were 30.5 by 54 by 2.6 nm. The upper and lower crystals were equally sized. The simulation was equilibrated at 300 K similarly to the single crystal and then loaded with compression along the x-direction. This favored twinning in both grains, but more in the upper grain. Loading at $10^8 s^{-1}$ was applied up to 1 GPa. The x-dimension was then held fixed, and the stress allowed to plastically dissipate. Time integration was done with a NVE ensemble.

For all simulations, OVITO [38] was used for visualization with potential energy and the basal plane vector [7] used for coloration.

Interfacial defect theory, developed by Pond and coworkers [39–43] and previously applied to hcp twinning by Serra [44–49], was used for characterization. This work was extended by Barrett and El Kadiri [32, 50] to characterize interactions between disclinations and disconnections on twin interfaces [30, 33, 51].

Results

Single Crystal Nucleation

Characterization of atomistic results is greatly improved by ready identification of the relevant planes and directions in raw atomistic data. To help the reader follow along with our analysis, we have produced the following key in Fig. 1 illustrating common planes and directions seen from a variety of view directions in hexagonal close-packed lattices.

Single crystal $\{10\bar{1}2\}$ twin nucleation in Mg generally occurs in the same manner regardless of whether free surfaces or periodic boundaries are used and regardless of the presence of initial voids or dislocations in the simulation [7]. In Fig. 2, we illustrate a small embryo which has just formed. Loading of Mg single crystals in tension on the c-axis prevents easy slip, leaving only pyramidal $<c+a>$ slip and $\{10\bar{1}2\}$ twinning as possible plastic mechanisms. In the MD timescale, $<c+a>$ slip nucleates more easily, at a tensile stress above 4GPa, which is a couple order of magnitude greater than the experimental yield for single crystals in this loading. It may be that there are alternate nucleation processes for $\{10\bar{1}2\}$ twins which require a greater activation time and thus are not observed here. In the scenario observed, $1/2<c+a>$ dislocations move across the lattice leaving a high-energy stacking fault. Then, a twin embryo forms on the fault which is faceted such that the directions $[1\bar{2}10]^{\text{parent}}$ and $[11\bar{2}3]^{\text{twin}}$ are aligned. Likewise, the directions $[1\bar{2}10]^{\text{twin}}$ and $[11\bar{2}3]^{\text{parent}}$ are aligned.

In Fig. 2, three facets are present with slightly different misorientations, and thus disclinations along their junctions. Two of them are $\{10\bar{1}1\}$ twist facets as discussed by [35]. These have a strained coherent character with a strain field imposing that $[2\bar{4}20]^{\text{parent}} = [11\bar{2}3]^{\text{twin}}$ and $[2\bar{4}20]^{\text{twin}} = [11\bar{2}3]^{\text{parent}}$. In our simulations, the facets were small and there were no misfit dislocations relieving this strain. The third facet is the BP facet which has been extensively

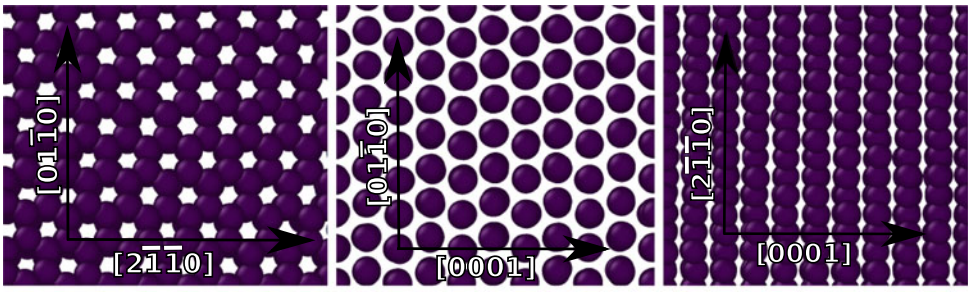

(a) $\langle 0\,0\,0\,1\rangle$ view normal (b) $\langle 2\,\bar{1}\,\bar{1}\,0\rangle$ view normal (c) $\langle 1\,0\,\bar{1}\,0\rangle$ view normal

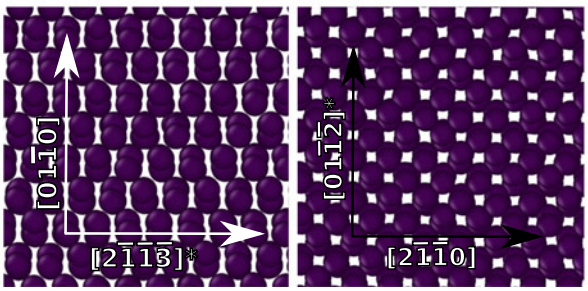

(d) $\langle 2\,\bar{1}\,\bar{1}\,3\rangle$ view normal (e) $\langle 1\,0\,\bar{1}\,2\rangle$ view normal

Fig. 1 Common view directions along with directions and plane normals visible in HCP lattices

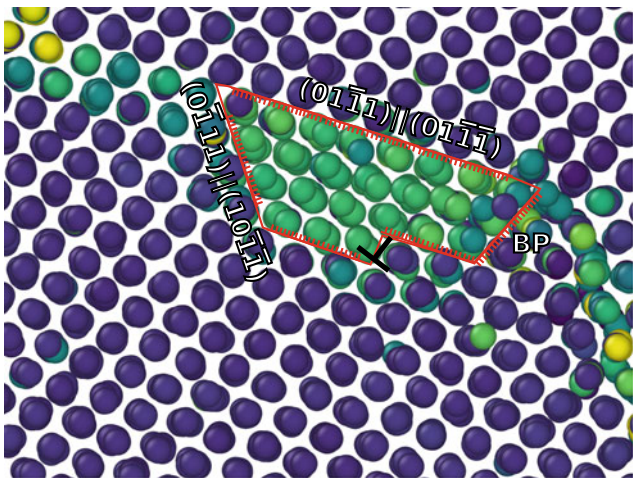

Fig. 2 $\{10\bar{1}2\}$ twin embryo viewed from the $<2\bar{1}\bar{1}0>$ plane growing off a $\{10\bar{1}1\}$ stacking fault. Inside the twin, the view direction is $<2\bar{1}\bar{1}3>$

discussed elsewhere [32]. A disconnection is seen moving on one of the $\{10\bar{1}1\}$ twist facets and growing the twin. Interfacial defect theory analysis suggests that this disconnection is glissile and can transform into a glissile disconnection on any of the other $\{10\bar{1}2\}$ twin facets.

The embryo seen here shows close resemblance with those shown in [7, 32]. As these embryos continue to grow, they adopt an ellipsoidal, roughly egg-shaped form. A transition to the more needle-shaped morphology seen experimentally is suggested in the largest simulations, but the simulation scale prevents a full transition to that shape.

Bi-crystal Nucleation

We also studied the case of grain boundary nucleation of $\{10\bar{1}2\}$ twins. These simulations were able to nucleate at much lower stresses and probably hold more relevance to experimental results. We appended the $\{1001\}$ and $\{10\bar{1}4\}$ planes of the upper and lower crystals to create a high-energy asymmetric tilt boundary. This orientation was chosen because it has a very high energy, but the interface between a $\{10\bar{1}2\}$ twin at the boundary with both the upper and lower grains should be low energy, thus enhancing the ease of nucleation. Figure 3 shows the nucleation process at several timesteps. These results are similar to earlier results by Wang et al. [52] for a symmetric tilt boundary with similar misorientation. Wang used a pileup of basal dislocations to encourage the nucleation process. In our work, no dislocations are present.

The initial very small embryos form during equilibration with no applied stress at all, illustrating the stability of the interfaces with the twin versus the low misorientation interface. Under applied load, the twins grow into both the upper and lower grains. These twin embryos show close to a needle-shaped morphology than the ones in single crystals. This is most likely because the misfit dislocations in the grain boundary discourage twin thickening.

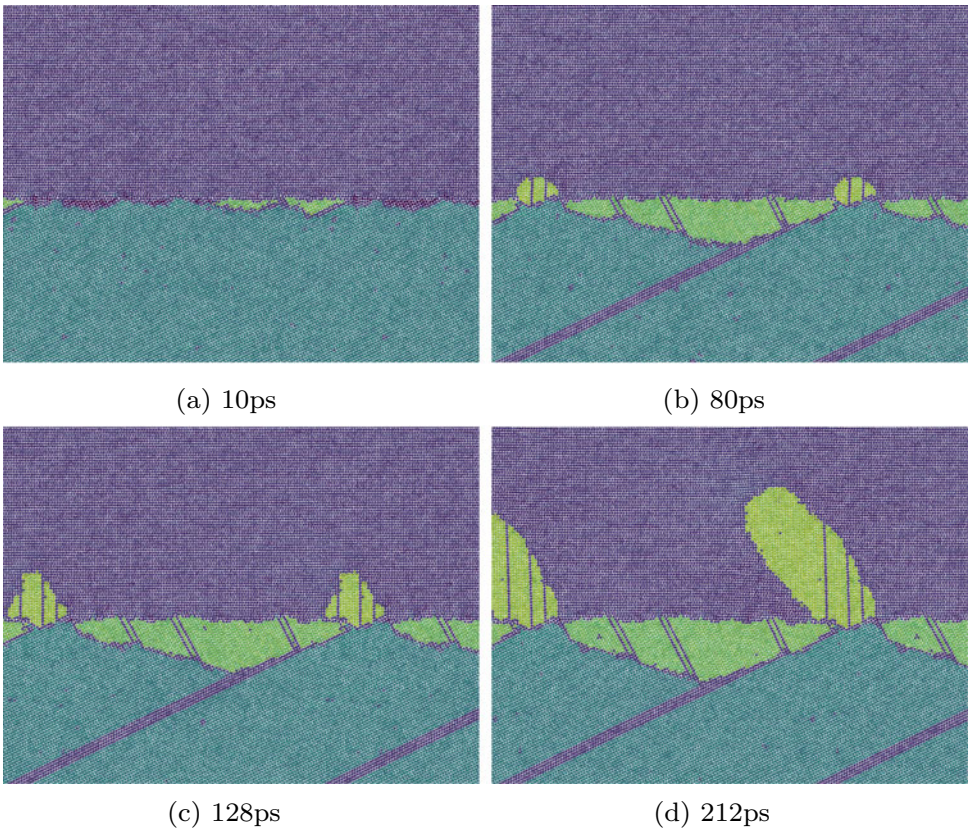

Fig. 3 A sequence of atomistic snapshots of the twin growing from the bi-crystal grain boundary. Twins inside the upper and lower grain are colored yellow–green and light green, respectively. Stripes through the twins are I_1 faults

The applied loading of x-axis compression favors growth of the upper grain. However, the lower grain initially grows faster. Evidently, the asymmetric nature of the grain boundary affects the relative propensity for twinning within the two grains.

Discussion

$\{10\bar{1}2\}$ Twin Embryo Morphology

The $\{10\bar{1}2\}$ twin nucleus makes extensive use of facets both within and outside of the shear plane. The role of these facets in the nucleation process is clearly critical. To help visualize the available facets in three dimensions, we have produced a schematic shown in Fig. 4. An embryo with all of these facets could appear to have an appearance like that of a cut gem. In a later publication, we will demonstrate that the formation and growth on all of these facets is interlinked and glissile movement of disconnections from one to another is permitted without any climb. The misorientations of most of the facets deviate from one another by 4° to 8°; thus, the facet junctions are delineated by disclinations. In larger embryos, we have studied such as those published in [32], the embryo did make use of most or all of these facets but because of the disconnection lines spanning around the embryo, it had more of a rounded appearance rather than having sharp boundaries like the schematic in Fig. 4. The increasing disclination dipole and coherency strain energies as the embryo grows tend to force the twin to adopt a single preferred boundary—either $(10\bar{1}2)$ or $(10\bar{1}\bar{2})$, which are the only two without any coherency strain. Thus, at larger scales, $\{10\bar{1}2\}$ twins are generally seen with primarily these boundaries. Still, in highly deformed samples, even larger twins may have misorientations which deviate from that of the ideal twin boundary [53], by making more use of basal-prismatic and prismatic-basal boundaries, for example.

Planar Nucleation of $\{10\bar{1}2\}$ Twins

By examining the details of the nucleation processes in both the single crystal and the bi-crystal cases, some common factors may be identified which we hypothesize play a critical role in $\{10\bar{1}2\}$ twin nucleation. The most important of these is that in both cases the $\{10\bar{1}2\}$ nucleated from a pre-existing planar defect. We propose that $\{10\bar{1}2\}$ do not generate from dissociation of a single dislocation line because that is not planar. Rather, a stacking fault or a grain boundary is necessary for the initial nucleation.

Furthermore, we propose that the orientation of this planar fault must coincide with one of the many facet planes of

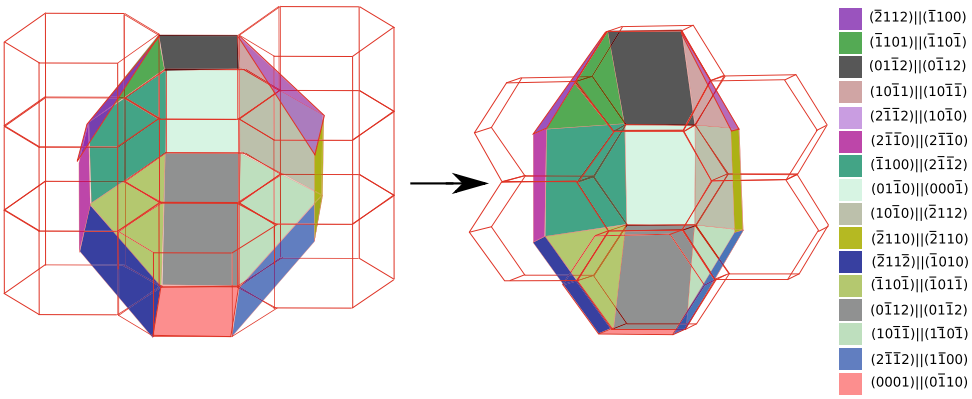

Fig. 4 Complete set of known facets for $\{10\bar{1}2\}$ twinning. The facets are capable of completely enclosing the embryo

the $\{10\bar{1}2\}$ twin. This requirement was fulfilled in both simulations—the single crystal case generated first-order $<c+a>$ partial dislocations leaving a stacking fault on the $\{10\bar{1}1\}$ plane. The $\{2112\}$ plane is also a facet plane for $\{10\bar{1}2\}$ twinning, so we theorize that second-order pyramidal $<c+a>$ slip could also produce a stacking fault from which a $\{10\bar{1}2\}$ twin originated. In the bi-crystal asymmetric tilt boundary, the local structure was composed of a couple of structural units, primarily appending $\{10\bar{1}2\}||\{10\bar{1}1\}$ planes and $\{10\bar{1}4\}||\{0001\}$ planes. Some $\{0001\}||\{10\bar{1}4\}$ local structures also appeared to be present. In any case, the twins nucleated from the basal planes move into both the upper and lower grains.

The final common factor in both simulations is that the nucleation of the twin provided significant energy relaxation compared to the pre-existing planar defect. In the bi-crystal case, this was so pronounced that the embryo formed with no applied load. It remained very small, only three layers thick, until loading was applied.

One of the primary difficulties in describing twin nucleation has been to explain a process which could reasonably produce the separation of the initial twinning disconnection dipole to form the first twinned region. In normal circumstance, there is a great attractive form driving the embryo to collapse. In our theory, the high-energy planar defect offsets this driving force by providing another driving force pushing the embryo to grow. Once the twin reaches the edge of the stacking fault, the trailing partial, or a misfit dislocation in the grain boundary, further energy relaxation by twin growth cannot be accomplished. Whether or not the nucleus grows into a full size twin then depends upon how large the embryo has grown and the applied stress state. In many scenarios, the embryo by this point will be larger than the critical size needed to shoot into the grain.

Conclusions

We performed molecular dynamics simulations to investigate the nucleation of $\{10\bar{1}2\}$ twins in Mg. Twins were nucleated in both single crystals and bi-crystals. Characterization of the twin embryos revealed that in both cases, twins nucleated on a pre-existing planar fault via faceting. The actual $(10\bar{1}2)$ twin boundary was not present in the initial embryos, hindering easy identification. We propose that $\{10\bar{1}2\}$ twins require a pre-existing high-energy planar defect to nucleate on one of the twin's faceting planes. In this scenario, the first 1–3 disconnection dipoles to form experience a driving force from the energy relaxation of the planar defect which overcomes their attractive nature and thus enables the embryo to stabilize. In scenarios where the applied loading is favorable and the embryo stabilizes above a critical size, shooting of $\{10\bar{1}2\}$ disconnections into the lattice can occur.

References

1. E. Orowan, AIME, New York p. 69 (1954)
2. P. Price, J. Appl. Phys. **32**(9), 1746 (1961)
3. J.W. Christian, *The Theory of Transformations in Metals and Alloys: Part I + II.* (Elsevier, 2002)
4. D. Oliver, Research **5**, 45 (1952)
5. N.P. Allen, B.E. Hopkins, J.E. McLennan, Proc. R. Soc. London, Ser. A **234**(1197), 221 (1956)
6. J.J. Cox, G. Horne, R. Mehl, T. Am. Soc. Metal **49**, 118 (1957)
7. C. Barrett, H. El Kadiri, M. Tschopp, J. Mech. Phys. Solids **60** (12), 2084 (2012). Cited By (since 1996) 0
8. R.L. Bell, R.W. Cahn, Proc. R. Soc. London, Ser. A **239**, 494 (1957)
9. R.W. Cahn, Il Nuovo Cimento (1943–1954) **10**, 350 (1953)

10. R.E. Reed-Hill, W.D. Robertson, Trans. Met. Soc. AIME **220**, 496 (1957)
11. A.M. Garde, E. Aigeltinger, R.E. Reed-Hill, Metall. Trans. B **4** (10), 2461 (1973)
12. R.E. Reed-Hill, in *The Inhomogeneity of Plastic Deformation*, ed. by R.E. Reed-Hill. American Society for Metals (American Society for Metals, Metals Park, OH, 1973), pp. 285–311
13. A.H. Cottrell, B.A. Bilby, Philos. Mag. Series 7 **42**(329), 573 (1951)
14. N. Thompson, D. Millard, Philos. Mag. **43**, 422 (1952)
15. S. Mendelson, J. Appl. Phys. **40**(4), 1988 (1969)
16. S. Mendelson, Mater. Sci. Eng. **4**(4), 231 (1969)
17. S. Mendelson, Nat. Bur. Stand. (US), Spec. Publ. **317**, 495 (1970)
18. S. Mendelson, J. Appl. Phys. **41**(5), 1893 (1970)
19. S. Mendelson, Scr. Metall. **4**(1), 5 (1970)
20. K.P.D. Lagerlöf, J. Castaing, P. Pirouz, A.H. Heuer, Philos. Mag. A **82**(15), 2841 (2002)
21. L. Capolungo, D. Spearot, M. Cherkaoui, D. McDowell, J. Qu, K. Jacob, Journal of the Mechanics and Physics of Solids **55**(11), 2300 (2007)
22. L. Capolungo, I. Beyerlein, Phys. Rev. B **78**(2), 024117 (2008)
23. L. Capolungo, I.J. Beyerlein, G.C. Kaschner, C.N. Tomé, Mater. Sci. Eng., A **513–514**, 42 (2009)
24. I.J. Beyerlein, C.N. Tomé, Proc. R. Soc. London, Ser. A **466** (2121), 2517 (2010)
25. I. Beyerlein, L. Capolungo, P. Marshall, R. McCabe, C. Tomé, Philosophical Magazine **90**(16), 2161 (2010)
26. J. Wang, I.J. Beyerlein, C.N. Tomé, Scr. Mater. **63**(7), 741 (2010)
27. J. Wang, R.G. Hoagland, J.P. Hirth, L. Capolungo, I.J. Beyerlein, C.N. Tomé, Scr. Mater. **61**, 903 (2009)
28. J. Wang, J.P. Hirth, C.N. Tomé, Acta Mater. **57**, 5521 (2009)
29. J. Wang, L. Liu, C. Tomé, S. Mao, S. Gong, Materials Research Letters **1**(2), 81 (2013)
30. A. Ostapovets, A. Serra, Journal of materials science **52**(1), 533 (2017)
31. C.D. Barrett, H. El Kadiri, Acta Materialia **63**, 1 (2014)
32. C.D. Barrett, H. El Kadiri, Acta Materialia **70**, 137 (2014)
33. H. El Kadiri, C.D. Barrett, J. Wang, C.N. Tomé, Acta Materialia **85**, 354 (2015)
34. A. Serra, D.J. Bacon, Philos. Mag. A **73**(2), 333 (1996)
35. Y. Liu, N. Li, S. Shao, M. Gong, J. Wang, R. McCabe, Y. Jiang, C. Tomé, Nature communications **7**, 11577 (2016)
36. S. Plimpton, J. Comput. Phys. **117**(1), 1 (1995)
37. X. Liu, J. Adams, F. Ercolessi, J. Moriarty, Modell. Simul. Mater. Sci. Eng. **4**, 293 (1996)
38. A. Stukowski, Modelling and Simulation in Materials Science and Engineering **18** (2010)
39. R. Pond, Philos. Mag. A **47**(6), 49 (1983)
40. R. Pond, W. Bollmann, Philosophical Transactions of the Royal Society of London. Series A, Mathematical and Physical Sciences **292**(1395), 449 (1979)
41. R. Pond, *Dislocations and Properties of Real Materials* (Institute of Metals, 1985), chap. Interfaces and dislocations, pp. 71–93
42. R. Pond, A. Bastaweesy, Le Journal de Physique Colloques **46** (C4), 4 (1985)
43. R. Pond, M. Aindow, W. Clark, Scr. Metall. **21**(7), 971 (1987)
44. A. Serra, D.J. Bacon, Philos. Mag. A **63**(5), 1001 (1991)
45. A. Serra, D.J. Bacon, R.C. Pond, Acta Metall. **36**, 3183 (1988)
46. A. Serra., R.C. Pond, D.J. Bacon, Acta Metall. Mater. **39**(7), 1469 (1991)
47. A. Serra, D.J. Bacon, Mater. Sci. Forum **126**, 69 (1993)
48. A. Serra, D.J. Bacon, Acta Metall. Mater. **43**(12), 4465 (1995)
49. A. Serra, D.J. Bacon, R.C. Pond, Metall. Mater. Trans. A **33**(3), 809 (2002)
50. C.D. Barrett, H. El Kadiri, Scripta Materialia **84**, 15 (2014)
51. F. Wang, C.D. Barrett, R.J. McCabe, H. El Kadiri, L. Capolungo, S.R. Agnew, Acta Materialia **165**, 471 (2019)
52. J. Wang, S. Yadav, J. Hirth, C. Tomé, I. Beyerlein, Materials Research Letters **1**(3), 1 (2013)
53. J. Zhang, S.P. Joshi, J. Mech. Phys. Solids **60**(5), 945 (2012)